Design of Compact Novel Dual-Band BPF Using Open-Loop Dumbbell Shaped Defected Ground Structure and Step Impedance Cross-Shaped Lines with Independently Controllable Frequencies and Bandwidths

R. Khosravi [1], Ch. Ghobadi [2], J. Nourinia [2], M. Abbasilayegh [2], and B. Mohammadi [2]

[1] Department of Electrical Engineering, Science and Research Branch
Islamic Azad University, West Azerbaijan, Iran
ronak62@gmail.com

[2] Department of Electrical Engineering
Urmia University, Urmia, Iran
ch.ghobadi@urmia.ac.ir, j.nourinia@urmia.ac.ir, m.abbasilayegh@urmia.ac.ir, b.mohammadi@urmia.ac.ir

Abstract ─ In this paper a compact novel dual-band bandpass filter (DB-BPF) with independently controllable frequencies and bandwidths is presented and the procedure of its design is discussed. The proposed filter consists of an open-loop dumbbell shaped (OLDS) defected ground structure (DGS) and step impedance cross-shaped lines (SICSLs). To generate the first band, the authors used a pair of end-coupled uniform transmission lines with equal-length on the top and an OLDS outline symmetrically was etched in the ground plane. In addition, by introducing cross-shaped lines, a dual band function is achieved. In the proposed structure, in order to reject the unwanted harmonic pass bands, step impedance transmission lines are implemented along the ports of the filter. The fabricated filter has the merits of simple topology, compact size, good return loss, low insertion loss and high isolation. The measurement agrees well with the simulation.

Index Terms ─ Defected Ground Structure (DGS), Dual-band Bandpass Filter (DB-BPF), Step Impedance Cross-Shaped Lines (SICSLs).

I. INTRODUCTION

Microstrip BPFs have been extensively studied and developed for a long time to meet various requirements in many modern communication systems. Among these designs, planar types of narrow and wide BPFs are highly promising in size compactness, large out-of-band rejection, low fabrication cost, and so on [1]–[18]. DB-BPFs are highly desired in modern dual-band wireless communication systems. Therefore, they have been extensively investigated and various design approaches have been proposed [1]–[14]. Among them, there are three typical methods. The first approach is using the cascade connection of a BPF and a bandstop filter. However, it occupies large size. The second method is utilizing stepped-impedance resonators (SIRs) as multi-mode resonators (MMRs), by controlling impedance and the length ratios of the SIRs, the desired operating frequencies can be obtained, the two resonant frequencies of which can be controlled by the impedance ratio and electrical length of two sections [1]–[5]. The third approach is using dual-mode DB-BPF [6]–[11]. [2] presents a compact DB-BPF based on mixed electric and magnetic coupling. SIR is utilized to construct mixed electric and magnetic coupling by placing the low impedance stubs and the high-impedance stubs closely, respectively. A transmission zero (TZ) can be generated and its location is determined by the dominant coupling.

In [4], compact dual-wideband function is achieved based on a novel penta-mode resonator (PMR). The first two modes are employed to generate the first passband, and the other three modes are used to form the second one. In [5], a compact dual-wideband BPF with two MMRs is proposed. The first MMR is a quad-mode resonator (QMR) which consists of a main transmission line loaded with a short-ended stub and two open-ended stubs, and the second MMR is a triple-mode resonator (TMR) which is composed of a main transmission line loaded with a square ring and a short-ended stub. In [3], a compact and high selectivity dual-band dual-mode microstrip BPF with the source-load coupling is proposed using the single short-circuited stub-loaded SIR. The resonator can generate two resonant modes in each band.

In general, dual-mode characteristics are excited by adding corner cut or corner patch perturbations to loop resonator. This pair of degenerate modes is coupled with each other and its coupling strength can be adjusted by the perturbation's size with respect to the

Submitted On: March 26, 2015
Accepted On: July 24, 2016

reference element. Patch perturbation with capacitive coupling is often adopted in dual-mode resonator filter because it can provide TZs for high selectivity design [6]–[11]. In [6], two microstrip perturbed ring resonators are employed to obtain dual-mode dual-band responses. [7] proposes a single slotted circular patch resonator for a dual-mode DB-BPF design. The arc- and radial-oriented slots are used to bring down the TM_{01}-like mode and to split the TM_{11}-like mode and its degenerate mode, respectively. [8] Presented a novel multilayer dual-mode DB-BPF using two identical microstrip cross-slotted patch resonators placed back-to-back. The lengths of the slots on the patch resonator are designed to be different, which can be used to control the two degenerate modes. Another class of dual-mode DB-BPFs can be realized by open-loop resonators and center-loaded resonators [9] or open-loop slotline resonators [10]. A perturbation technique using simple loading stub is investigated in [10], which is applied to produce the non-degenerate mode for open-loop slotline resonator and to improve the operating band selectivity. The distinct characteristics of this dual-mode resonator are studied by using even–odd mode analysis. Likewise, equivalent circuit models at non-degenerate modes are given to determine the resonance frequencies and TZs. In [11] a simple microstrip ring-resonator is presented for novel design of dual-band dual-mode BPFs. By increasing the length of the loaded open-circuited stub, the two first-order degenerate modes are excited and slit for the use of the first passband. Moreover, other strategies to improve the impedance bandwidth which do involve a modification of the geometry of the planar DB- BPFs have been investigated in [12]-[14].

In this paper, a compact novel DB-BPF with independently controllable frequencies and bandwidths has been presented. The proposed DB-BPF consists of OLDS DGS and SICSLs. By inserting an OLDS slot in the ground plane and a pair of end-coupled uniform transmission lines with equal-length on the top, the first band can be produced.

The OLDS slot consists of two identical circle loops having open-loop edge length (W_{10}-W_{11}) together with open ends W_9 and a slot-line L_8 which forms connection between them. In this configuration, the dumbbell-arm is aligned with the microstrip line on the top. Placing OLDS slot in the ground plane is used for miniaturizing the size of proposed structure and also improving the mutual coupling between the end-coupled transmission lines. In addition, by introducing cross-shaped lines, a dual band function is achieved. By step impedance transmission lines, significant improvement in isolation between dual-band is observed. Also by using OLDS DGS, much wider bandwidth can be produced. In addition, a parametric study is carried out in detail to provide filter engineers with essential design information. The experimental data show that the DB-BPF can provide two band-widths of 920 MHz centered at 3 GHz and 830 MHz centered at 8 GHz.

II. DB-BPF DESIGN AND CONFIGURATION

The compact novel DB-BPF with independently controllable frequencies and bandwidths fed by a 50Ω microstrip lines is shown in Fig. 1, which is printed on a Rogers (RO4003) substrate of thickness 0.8 mm, permittivity 3.55, and loss tangent 0.0027. The basic DB-BPF structure consists of OLDS DGS and SICSLs. The transmission lines are connected to a feed line of width W_1 and length L_1, as shown in Fig. 1. The proposed DB-BPF is connected to a 50Ω SMA connector for signal transmission. A single band function is provided by inserting an OLDS slot in the ground plane and a pair of end-coupled uniform transmission lines with equal-length on the top and a dual band characteristic is obtained by introducing cross-shaped lines. The end-coupled transmission lines provide one TZ at DC. The first passband is further bounded by two finite TZs at frequencies lower TZ (1.06 GHz) and upper TZ (3.91 GHz) because of OLDS DGS. The first passband of the measured results is centered at 3 GHz with a low insertion loss of 1 dB and an FBW of 31%. The second passband of the measured results has a center frequency of 8 GHz with a low insertion loss of 2 dB, and an FBW of 11%. The planar DB-BPF with various design parameters is constructed, and the numerical and experimental results of the input impedance and transmission characteristics are presented and discussed. The parameters of this proposed DB-BPF are studied by changing one parameter at a time and fixing the others. The simulated results are obtained using Ansoft simulation software high-frequency structure simulator (HFSS). The final values of the presented DB-BPF design parameters are specified in Table 1.

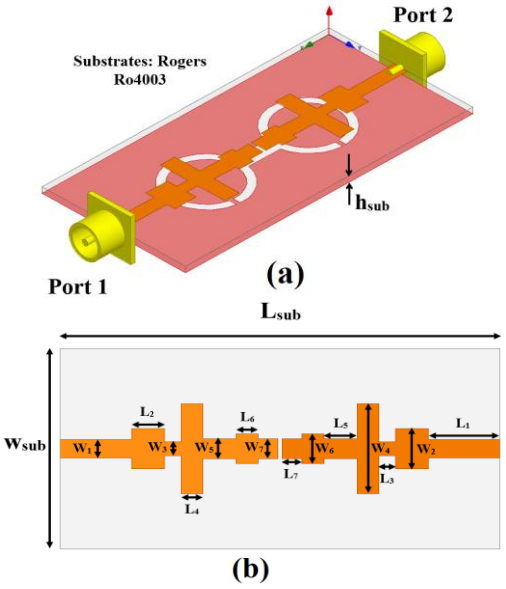

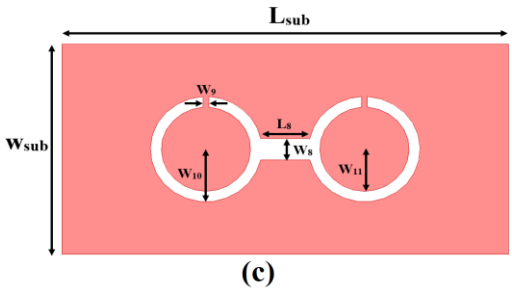

Fig. 1. The Geometry of the proposed DB-BPF using OLDS and SICSLs: (a) side view, (b) top view, and (c) bottom view.

Table 1: The final values of design parameters

Param.	mm	Param.	mm	Param.	mm
W_{sub}	20	W_7	2	L_2	3
W_1	1.8	W_8	2	L_3	1.5
W_2	4	W_9	0.5	L_4	2
W_3	1.4	W_{10}	5	L_5	3
W_4	9	W_{11}	4	L_6	2
W_5	2	L_{sub}	40	L_7	1.8
W_6	3	L_1	6.5	L_8	4.2

Figure 2 shows the structure of various microstrip filters which are used for simulation studies. Frequency responses for filter with OLDS DGS and a pair of end-coupled uniform transmission lines (Fig. 2 (a)), with a pair of end-coupled uniform transmission lines and cross-shaped lines (Fig. 2 (b)), and the proposed structure are compared in Fig. 3. As shown in Fig. 3, for the proposed DB-BPF configuration, in order to generate the first band characteristics, an OLDS slot is used in the ground plane and a pair of end-coupled uniform transmission lines with equal-length on the top and by introducing cross-shaped lines; a dual band function is achieved that covers all the 2.61-3.53 GHz and 7.82-8.65 GHz for WLAN/WiMAX and satellite communications, respectively.

As illustrated in Fig. 3, the passband is bounded by two TZs. One is at DC and the other at some higher frequency. The zero at DC is imposed by the end-coupled line (gap width= 0.4 mm) whilst the higher-frequency TZ is generated by the above DGS pattern. To improve the stopband performance of the above filter using OLDS DGS, step impedance transmission lines can be considered. In general, the OLDS DGS perturbs the current distribution on the ground plane of the microstrip line and as a result the equivalent inductance and capacitance are increased. The dimensions of the OLDS DGS have influence on its frequency behavior as by increasing the area of the DGS the cutoff frequency decreases and the attenuation pole moves toward lower frequencies. In order to explain the movement of the attenuation pole toward the lower frequencies, it can be said that by increasing the area of the defect structure the length of the looping path around the OLDS DGS for the returning current on the ground plane is increased and as a result the effective inductance of the transmission line is increased which in turn leads to an increase in equivalent inductance of the overall structure and consequently the cutoff frequency is decreased and the attenuation pole is moved toward lower frequencies [15]–[17].

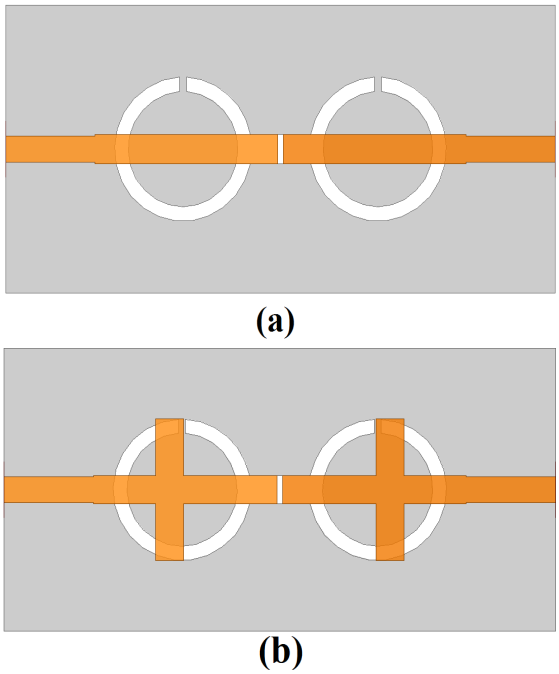

Fig. 2. Filter with OLDS DGS and (a) a pair of end-coupled uniform transmission lines, (b) a pair of end-coupled uniform transmission lines and cross-shaped lines.

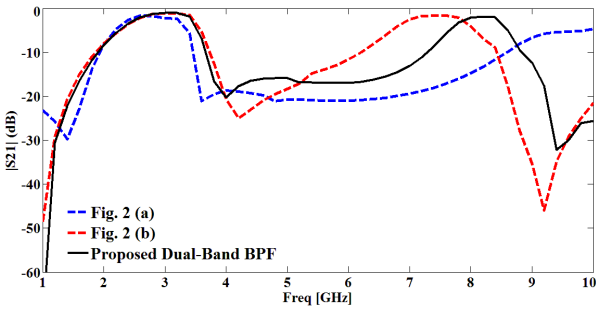

Fig. 3. The insertion loss characteristics for filter structures shown in Fig. 2 and proposed DB-BPF.

In order to modify the design parameters of the proposed DB-BPF, a parametric study was performed. As examples of the aforementioned parametric study, the effect of five design parameters are presented and

discussed here. Figure 4 shows the effect of variation in inner radius length of the OLDS DGS (W_{11} in Fig. 1 (c)) on the frequency responses of the proposed DB-BPF for different cases. It is found that by changing the inner radius length of the OLDS DGS from 3.0 mm to 4.5 mm, the position of the attenuation pole is shifted from 4.2 GHz to 3.7 GHz, respectively. Fig. 5 shows the effect of variation in outer radius length of the OLDS DGS (W_{10} in Fig. 1 (c)) on return loss characteristic of the proposed DB-BPF for different cases. As can be observed from this figure, the impedance bandwidth can be fine-tuned effectively by modifying this parameter. Another effective way to tune the proposed DB-BPF is the replacement of uniform transmission by SICSLs.

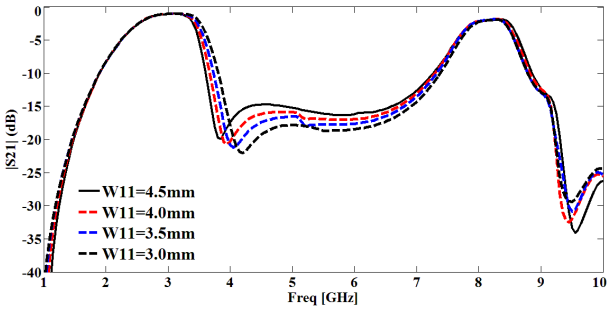

Fig. 4. The effect of variation in inner radius length of the OLDS DGS (W_{11} in Fig. 1 (c)) on insertion loss.

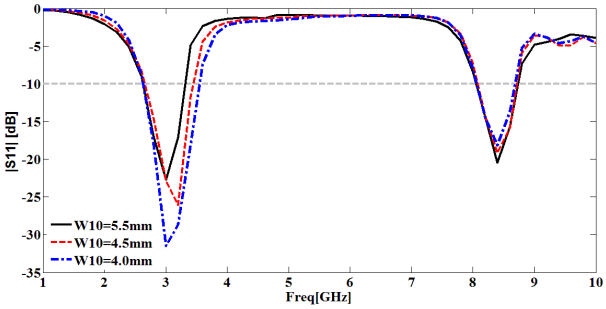

Fig. 5. The effect of variation in outer radius length of the OLDS DGS (W_{10} in Fig. 1 (c)) on return loss.

Figure 6 shows the effect of variation in the width of the arm of the SICSLs (L_6 in Fig. 1 (b)) on return loss. From the simulation results in Fig. 6, it can be seen in the figure that the impedance bandwidth and return loss characteristics of the upper frequency band are slightly changed when L_6 is varied. The simulated return loss curves with different values of the proposed DB-BPF are plotted in Fig. 7. From the simulation results in Fig. 7, it is found that the upper frequency band is significantly affected by the variation of the W_4.

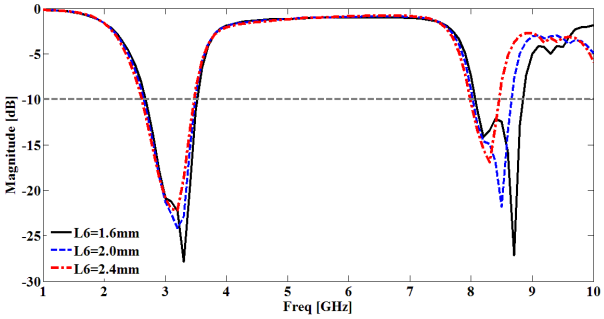

Fig. 6. The effect of variation in the width of the arm of the SICSLs (L_6 in Fig. 1 (b)) on return loss.

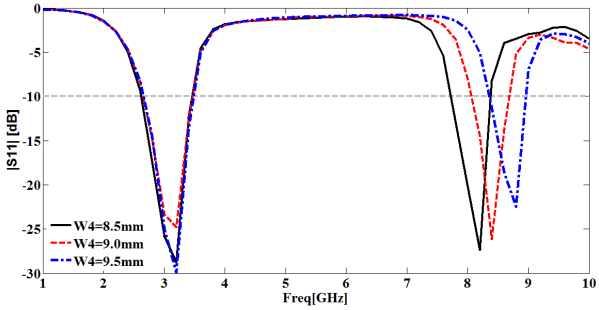

Fig. 7. The effect of variation in the finger length of the vertical arm of the cross-shaped lines (W_4 in Fig. 1 (b)) on return loss.

As illustrated in Fig. 8, the upper passband is bounded by a TZ at upward 9 GHz that is imposed by the cross-shaped lines. To improve the stopband performance of the upper passband, step impedance transmission lines can be considered. It is found that by changing the finger width of the vertical arm of the cross-shaped lines (L_4 in Fig. 1 (b)) from 1.4 mm to 2.4 mm, the position of the proposed TZ is shifted from 9.85 GHz to 9.07 GHz, respectively.

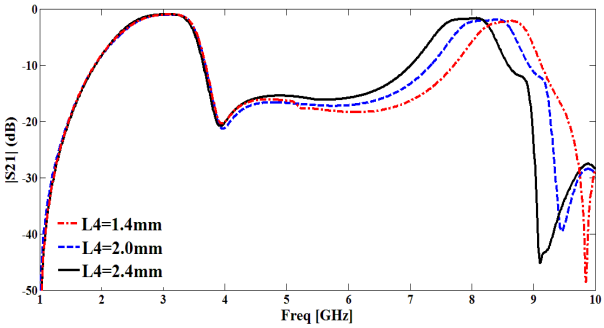

Fig. 8. The effect of variation in the finger width of the vertical arm of the cross-shaped lines (L_4 in Fig. 1 (b)) on insertion loss.

III. RESULTS AND DISCUSSIONS

The proposed DB-BPF with final design parameters, as shown in Fig. 9, was fabricated and tested. All measured and simulated results of the fabricated DB-BPF are shown in Fig. 10. The first passband of the measured results is centered at 3.07 GHz (2.61-3.53 GHz) with a low insertion loss of 1 dB, a return loss of 20 dB, and an FBW of 31%. The second passband of the measured results has a central frequency of 8.23 GHz (7.82-8.65 GHz) with a low insertion loss of 2 dB, a return loss of 16 dB and a FBW of 11%. The three TZs are located at 1.06, 3.91, and 9.74 GHz with attenuation levels of 40, 21, and 35 dB, respectively.

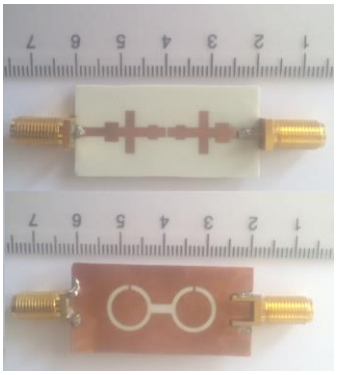

Fig. 9. Photograph of the fabricated DB-BPF prototype with OLDS and SICSLs.

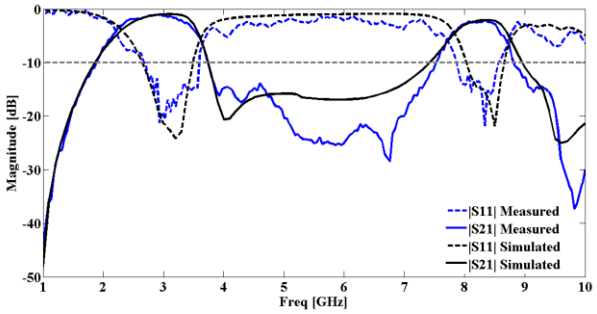

Fig. 10. Measured and simulated frequency responses of the fabricated DB-BPF using OLDS and SICSLs shown in Fig. 1.

The measured results show a good performance, which verifies the design concepts. As shown in the measured results, there exists a discrepancy between the measured data and the simulated results. The discrepancy is mostly due to a number of parameters such as the fabricated DB-BPF dimensions as well as the thickness and dielectric constant of the substrate, on which the DB-BPF is fabricated. In order to confirm the accurate return loss characteristics for the designed DB-BPF, it is recommended that the manufacturing and measurement process need to be performed carefully; besides, SMA soldering accuracy and substrate quality need to be taken into consideration [18]-[20]. In summary it can be said that a fine agreement between measured and simulated results is obtained in the frequency band of operation. Finally, a comparison between the proposed DB-BPF and other filter structures which have been published in literature and used here as references is presented in Table 2. From this table it can be concluded that the proposed DB-BPF has improved in-band and out-of-band performances as well as size miniaturization. In comparison with [3, 10, 11] and [13], the proposed DB-BPF has a smaller size, with respect to the operating frequency band and substrate relative dielectric constant. The presented DB-BPF has a wider bandwidth in comparison with the DB-BPFs in [1], [3] and [10]-[11]. The transmission loss performance of the presented DB-BPF is better than the ones in [1] and [10]. The in-band performance of the presented DB-BPF is better than the ones in [3], [5]. Moreover, the realization of the proposed DB-BPF is simpler than the ones in [1, 4, 5, 13].

IV. CONCLUSION

A compact novel DB-BPF with independently controllable frequencies and bandwidths are presented and discussed. The proposed DB-BPF consists of OLDS DGS and SICSLs. By inserting an OLDS slot in the ground plane and a pair of end-coupled uniform transmission lines with equal-length on the top, the first band can be produced. In addition, by introducing cross-shaped lines, a dual band function is achieved. In the proposed structure, in order to reject the unwanted harmonic pass bands, step impedance transmission lines are implemented along the ports of the filter. The DB-BPF exhibits low insertion loss over the desired passbands, and a sufficient isolation level at the frequency bands of interest.

Table 2: A comparison among the proposed DB-BPF using OLDS and SICSLs and the previous works

Ref.	f_0 (GHz)	IL (dB)	FBW (%)	ε_r/h (mm)	Size (mm^2)
[1]	2.37/3.43	2.85/2.94	7/1	3.5/0.508	137
[2]	2.58/6.79	0.54/1.18	44.7/18.3	2.2/0.508	132
[3]	1.58/5.2	1.6/1.42	4/3	2.2/0.508	470
[4]	3.32/5.32	0.62/0.91	28/20	3.55/0.508	218
[5]	2.34/3.46	0.84/1.2	26/21	3.38/0.508	258
[9]	3.88/5.35	0.38/1.03	12.4/8.6	2.54/0.54	276
[10]	3.34/3.93	1.8/1.9	5.2/7.7	4.5/0.8	232
[11]	2.3/4.1	0.65/1.0	11/8	10.8/1.27	339
[13]	1.03/2.85	0.65/0.45	94.8/35.8	10.8/1.27	306
This Work	3.07/8.23	0.8/1.8	31/11	3.55/0.8	480

f_0: Centre frequency of operation bands; IL: Insertion Loss over the whole pass-bands; ε_r: substrate relative dielectric constant; h: substrate thickness.

ACKNOWLEDGMENT

The authors thank the northwest antenna and microwave research laboratory (NAMRL) for their beneficial and professional help.

REFERENCES

[1] Y. Mo, K. Song, and Y. Fan, "Compact dual-band bandpass filter based on mixed electric and magnetic coupling," *Microwave and Optical Technology Letters*, vol. 56, pp. 1903-1907, August 2014.

[2] H. J. Xu and W. Wu, "Miniaturised dual-wideband bandpass filter using novel dual-band coupled-line sections," *Electronics Letters*, vol. 49, no. 18, pp. 1162-1163, August 2013.

[3] J. Li, Sh. Huang, and J. Z. Zhao, "Compact dual-wideband bandpass filter using a novel penta-mode resonator (PMR)," *IEEE Microw. Wireless Compon. Lett*., vol. 24, no. 10, pp. 668-670, October 2010.

[4] J. Li, Sh. Huang, H. Wang, and J. Z. Zhao, "A novel compact dual-wideband bandpass filter with multi-mode resonators," *Progress In Electro-magnetics Research Letters*, vol. 51, pp. 79-85, 2015.

[5] X. S. Zhang, B. Liu, Y. J. Zhao, J. K. Wang, and W. Chen, "Compact and high selectivity dual-band dual-mode microstrip BPF with five transmission zeros," *Microwave and Optical Technology Letters*, vol. 54, pp. 79-81, January 2012.

[6] X. Y. Zhang and Q. Xue, "Novel dual-mode dual-band filters using coplanar-waveguide-fed ring resonators," *IEEE Trans. Microw. Theory Tech*., vol. 55, no. 10, pp. 2183-2190, October 2007.

[7] R. Zhang, L. Zhu, and S. Luo, "Dual-mode dual-band bandpass filter using a single slotted circular patch resonator," *IEEE Microw. Wireless Compon. Lett*., vol. 22, no. 5, pp. 233-235, May 2012.

[8] J.-X. Chen, C. Shao, J. Shi, and Z.-H. Bao, "Multilayer independently controllable dual band bandpass filter using dual-mode slotted-patch resonator," *Electronics Letters*, vol. 49, no. 9, pp. 605-607, April 2013.

[9] Z. Yao, C. Wang, and N. Y. Kim, "A compact dual-mode dual-band bandpass filter using stepped impedance open-loop resonators and center-loaded resonators," *Microwave and Optical Technology Letters*, vol. 55, pp. 3000-3005, December 2013.

[10] H. Liu, L. Shen, L. Y. Shi, Y. Jiang, X. Guan, and T. Wu, "Dual-mode dual-band bandpass filters design using open-loop slotline resonators," *IET Microwave and Antenna Propagation*, vol. 7, no. 12, pp. 1027-1034, July 2011.

[11] S. Sun, "A dual-band bandpass filter using a single dual-mode ring resonator," *IEEE Microw. Wireless Compon. Lett*., vol. 21, no. 6, pp. 298-300, June 2011.

[12] X. Y. Zhang, C. H. Chan, Q. Xue, and B. J. Hu, "Dual-band bandpass filter with controllable bandwidths using two coupling paths," *IEEE Microw. Wireless Compon. Lett*., vol. 20, no. 11, pp. 616-618, November 2010.

[13] R. Zhang and L. Zhu, "Synthesis and design of dual-wideband bandpass filters with internally-coupled microstrip lines," *IET Microwave and Antenna Propagation*, vol. 8, no. 8, pp. 556-563, August 2014.

[14] Y. Wu, S. Zhou, W. Zhang, M. Liao, and Y. Liu, "Coupled-line dual-band bandpass filter with compact structure and wide stopband," *Electronics Letters*, vol. 50, no. 3, pp. 187-189, January 2014.

[15] S. Nouri, J. Nourinia, N. Valizade, B. Mohammadi, and A. Valizade, "Novel compact branch-line coupler using non-uniform folded transmission line and shunt step impedance stub with harmonics suppressions," *Applied Computational Electromagnetic Society (ACES) Journal*, vol. 31, no. 4, pp. 401-409, April 2016.

[16] B. Mohammadi, A. Valizade, J. Nourinia, and P. Rezaei, "Design of a compact dual-band-notch UWB bandpass filter based on wave cansellation method," *IET Microwave and Antenna Propagation*, vol. 9, no. 1, pp. 1-9, January 2015.

[17] B. Mohammadi, A. Valizade, P. Rezaei, and J. Nourinia, "A new design of compact dual band-notch UWB BPF based on coupled wave canceller inverted T-shaped stubs," *IET Microwave and Antenna Propagation*, vol. 9, no. 1, pp. 64-72, January 2015.

[18] B. Mohammadi, J. Nourinia, C. Ghobadi, and A. Valizade, "Design and analysis of the stub and radial-stub loaded resonator bandpass filter with cross-shaped coupled feed-lines for UWB applications," *Applied Computational Electro-magnetic Society (ACES) Journal*, vol. 28, no. 9, pp. 851-857, September 2013.

[19] P. Beigi, J. Nourinia, B. Mohammadi, and A. Valizade, "Bandwidth enhancement of small square monopole antenna with dual band notch characteristics using U-shaped slot and butterfly shape parasitic element on backplane for UWB applications," *Applied Computational Electro-magnetic Society (ACES) Journal*, vol. 30, no. 1, pp. 78-85, January 2015.

[20] S. Hoseyni, J. Nourinia, C. Ghobadi, S. Masumina, and B. Mohammadi, "A compact design and new structure of monopole antenna with dual band notch characteristic for UWB applications," *Applied Computational Electromagnetics Society Journal (ACES)*, vol. 31, no. 7, pp. 797-805, July 2016.

Ronak Khosravi received the B.Sc. degree in Electronic Engineering from Azad university of Tabriz in 2011 and M.Sc. degree in Telecommunications Engineering in Science and Research University of Urmia in 2014. Her interest include in wideband passive microwave devices and metamaterial antennas.

Changiz Ghobadi received his B.Sc. in Electrical Engineering-Electronics and M.Sc. degrees in Electrical Engineering from Isfahan University of Technology, Isfahan, Iran and Ph.D. degree in Electrical-Telecommunication from University of Bath, Bath, UK in 1998. From 1998 he was an Assistant Professor and now he is a Professor in the Department of Electrical Engineering of Urmia University, Urmia, Iran. His primary research interests are in antenna design, radar and adaptive filters.

Javad Nourinia received his B.Sc. in Electrical and Electronic Engineering from Shiraz University, M.Sc. degree in Electrical and Telecommunication Engineering from Iran University of Science and Technology, and Ph.D. degree in Electrical and Telecommunication from University of Science and Technology, Tehran Iran in 2000. From 2000 he was an Assistant Professor and now he is a Professor in the Department of Electrical Engineering of Urmia University, Urmia, Iran. His primary research interests are in antenna design, numerical methods in electromagnetic, microwave circuits.

Bahman Mohammadi received the B.Sc. degree in Electrical Engineering - Telecommunication from Tabriz University, Tabriz, Iran, in 2011 and M.Sc. degree in Electrical Engineering-Microwave, Antenna and Propagation from Urmia University, Urmia, Iran, in 2013 (1 honor or award). He is with Northwest Antenna and Microwave Research Laboratory (NAMRL) as a Microwave Engineering since March 2011. He has authored and co-authored more than 32 journal and conference papers. His research interests include Floquet Analysis and Periodic Structures, Microwave Components, Optimization Methods, MIMO and Measurements.